

Exotic break-up modes in heavy ion reactions up to Fermi energies*Maria Colonna,^{1,†} Virgil Baran,² Stefano Burrello,¹ Mariangela Di Prima,¹ Paolo Napolitani,³ and Carmelo Rizzo¹¹*INFN-Laboratori Nazionali del Sud, Via S Sofia 62, Catania I-95123, Italy*²*NIPNE-HH, Bucharest University, Bucharest 077125, Romania*³*IPN, CNRS/IN2P3, Université Paris-Sud 11, Orsay cedex 91406, France*

(Received January 8, 2015; accepted in revised form January 17, 2015; published online April 20, 2015)

We discussed recent studies, within the framework of transport theories, on heavy ion reactions between charge asymmetric systems, from low up to Fermi energies. We concentrated on the analysis of ternary breakup events of dynamical origin occurring in semi-central reactions, where the formation of excited systems in various conditions of shape, excitation energy and spin is observed. At beam energies around 20A MeV, we showed how this fragmentation mode emerges from the combined action of surface (neck) instabilities and angular momentum effects, leading to the observation of three aligned massive fragments in the exit channel. At Fermi energies, a transition towards a prompt emission of small fragments from the neck region with larger relative velocity with respect to projectile and target remnants is observed. We also focus on isospin sensitive observables, aiming at extracting information on the density dependence of the isovector part of the nuclear effective interaction and of the nuclear symmetry energy.

Keywords: Low and intermediate energy heavy-ion reactions, Fluctuation phenomena, Equation of State

DOI: [10.13538/j.1001-8042/nst.26.S20509](https://doi.org/10.13538/j.1001-8042/nst.26.S20509)**I. INTRODUCTION**

The behavior of nuclear matter in several conditions of density, temperature and N/Z asymmetry is of fundamental importance for the understanding of many phenomena involving nuclear systems and astrophysical compact objects. This information can be accessed by means of heavy ion collision experiments, where transient states of nuclear matter spanning a large variety of regimes can be created. Actually this study allows one to learn about the corresponding behavior of the nuclear effective interaction, which provides the nuclear Equation of State (EOS) in the equilibrium limit. In particular, many investigations are concentrated nowadays on the EOS of asymmetric matter (Asy-EOS), which has, comparatively to the symmetric EOS [1], few experimental constraints.

We stress that the latter information is essential for the understanding of some important properties of neutron stars, whose crust behaves as low-density asymmetric nuclear matter [2, 3] and whose core may touch extreme values of density and asymmetry. Moreover, the low-density behavior of the symmetry energy also affects the structure of exotic nuclei and the appearance of new features involving the neutron skin, which are currently under intense investigation [4].

Over the past years, several observables which are sensitive to the nuclear EOS and testable experimentally, have been suggested. In this article, we will present some recent transport theory results on dissipative collisions, in a range of beam energies from just above the Coulomb barrier up to the Fermi energy regime, mainly concentrating on reaction mechanisms occurring at semi-central impact parameters. We

focus on new, exotic, break-up modes, showing how the fragmentation mechanism reflects the delicate balance between mean-field dynamics, associated shape and volume fluctuations and rotational effects. Moreover, fragment isotopic properties appear quite sensitive to the low-density behavior of the nuclear symmetry energy.

II. TRANSPORT THEORIES AND EFFECTIVE INTERACTIONS

Nuclear reactions are modeled by solving transport equations based on mean field theories, with short range (2p-2h) correlations included via hard nucleon-nucleon elastic collisions and via stochastic forces, selfconsistently evaluated from the mean phase-space trajectory [5].

In the energy range up to a few hundred A MeV, the appropriate tool is the so-called Boltzmann-Langevin (BL) equation [6]

$$\frac{df}{dt} = \frac{\partial f}{\partial t} + \{f, H\} = I_{\text{coll}}[f] + \delta I[f], \quad (1)$$

where $f(\mathbf{r}, \mathbf{p}, t)$ is the one-body distribution function, the semi-classical analog of the Wigner transform of the one-body density matrix, $H(\mathbf{r}, \mathbf{p}, t)$ is the mean field Hamiltonian, I_{coll} is the two-body collision term incorporating the Fermi statistics of the particles, and $\delta I[f]$ is its fluctuating part.

Several approximate treatments of the BL equation have been introduced so far. For instance, in BUU-like models, the fluctuating term $\delta I[f]$ is neglected [7], whereas in the Stochastic Mean Field (SMF) model [8] fluctuations are projected onto the coordinate space and are implemented agitating the spatial density profile.

Effective interactions (associated with a given EOS) can be considered as an input of all transport codes and from the comparison with experimental data one can finally get some hints on nuclear matter properties.

* Supported by a grant of the Romanian National Authority for Scientific Research, CNCS - UEFISCDI (No. PN-II-ID-PCE-2011-3-0972)

† Corresponding author, colonna@lns.infn.it

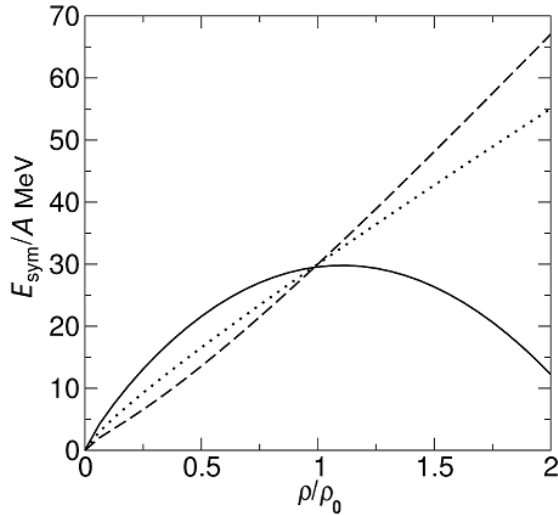


Fig. 1. Three effective parameterizations of the symmetry energy: asystiff (dotted line), asysoft (full line) and asysuperstiff (dashed line).

Unless specified, we adopt a soft isoscalar EOS (compressibility $K = 200$ MeV) and the free nucleon-nucleon cross section in the collision integral. We notice that the considered compressibility value is favored, e.g. from flow, monopole oscillation and multifragmentation studies [9, 10]. The choice considered corresponds to a Skyrme-like effective interaction, namely SKM*, for which we take the effective mass as being equal to the nucleon bare mass.

The symmetry energy $\frac{E_{\text{sym}}}{A} = \frac{E_{\text{sym}}}{A}(\text{kin}) + \frac{C(\rho)}{2\rho_0}\rho$ appears in the energy density functional $\epsilon(\rho, \rho_i) \equiv \epsilon(\rho) + \rho \frac{E_{\text{sym}}}{A}(\rho_i/\rho)^2 + O(\rho_i/\rho)^4 + \dots$, expressed in terms of total ($\rho = \rho_p + \rho_n$) and isospin ($\rho_i = \rho_p - \rho_n$) densities, from which the mean-field potential can be consistently derived (ρ_0 denotes the saturation density).

For some of the reaction mechanisms analyzed, the sensitivity of the simulation results is tested against different choices of the density dependence of the isovector part of the effective interaction. For instance, the symmetry energy behavior associated with three different parameterizations of $C(\rho)$ (the asysoft, the asystiff and asysuperstiff) is displayed in Fig. 1, detailed description is provided in [5]. Eq.(1) is solved numerically by adopting the test particle method [11].

Within our framework, the system is described in terms of the one-body distribution function f , but this function may experience a stochastic evolution in response to the action of the fluctuating term $\delta I[f]$. Then the model is suitable to treat the occurrence of instabilities and bifurcations of trajectories in nuclear dynamics.

III. FRAGMENTATION AT LOW ENERGY: TERNARY BREAKUP

We discuss semi-peripheral heavy ion collisions in the beam energy range of 10–30A MeV, focusing on the possi-

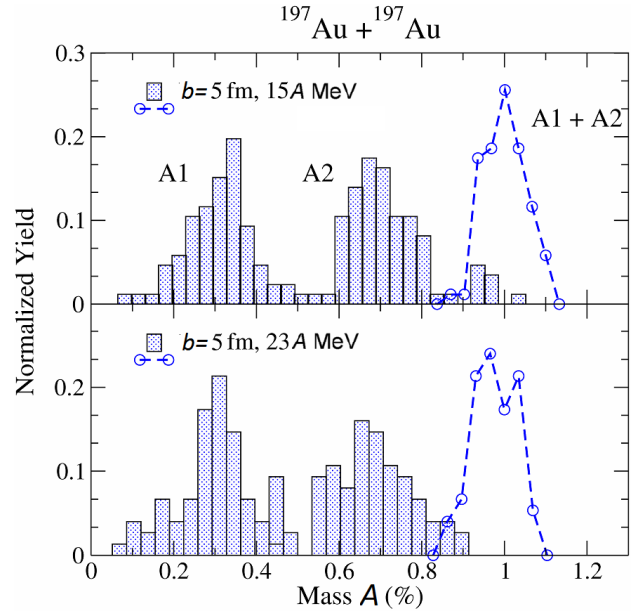


Fig. 2. (Color online) Mass distribution of the fragments A1 and A2, and of their sum, emerging from the breakup of the PLF/TLF fragment, for the reaction $^{197}\text{Au} + ^{197}\text{Au}$ at 15 and 23A MeV. A1 denotes the smallest fragment. Masses are normalized to the average mass of the PLF/TLF fragment.

ble occurrence of ternary breakup processes and on the features of the associated reaction products. Recent experimental investigations have been concentrated on these exotic separation modes, in the case of Au + Au reactions at 15 and 23A MeV [12–14].

Calculations are performed with the SMF approach. Let us consider first the reaction at 15A MeV, $b = [4-6]$ fm. In this case, we observe an almost symmetric neck rupture between projectile-like (PLF) and target-like (TLF) fragments, leading to the formation of two deformed fragments in the majority of the events. Important quadrupole and octupole deformations are noticed for the primary PLF/TLF fragments, which may lead to subsequent ruptures (multiple breakup) and, in particular, to ternary breakup events, caused by surface instabilities. An early fragment recognition method is applied to identify the most probable breakup configuration of the PLF (or TLF) fragment.

Figure 2 (top panel) shows the mass distribution of the lightest, A1, and heaviest, A2, fragments for the impact parameter $b = 5$ fm. Once the masses are normalized to the average mass of the PLF (or TLF) fragment, the results look in good agreement with experimental data [12]. In particular, the calculations are able to reproduce the distance between the A1 and A2 centroids and the variance of the mass distribution. Similar results have been recently reported in the context of the improved QMD (ImQMD) calculations of Ref. [15], where a detailed comparison with the experimental findings of Ref. [12] is presented. Results obtained at the higher bombarding energy of 23A MeV are shown in the bottom panel of the figure. The behavior observed for the mass distribution of fragments A1 and A2 is quite close to the one

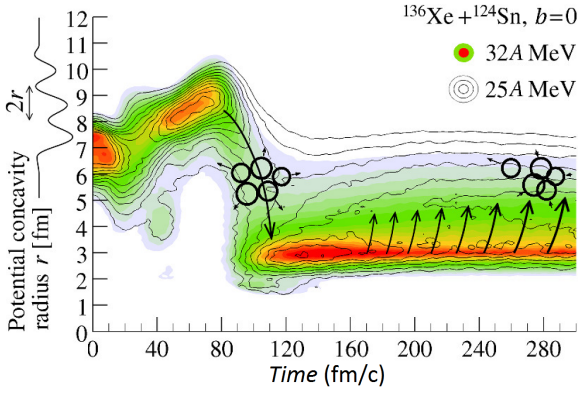


Fig. 3. (Color online) Calculation (BLOB) of the evolution of the size of inhomogeneities developing in the potential landscape as a function of time for the reaction $^{136}\text{Xe} + ^{124}\text{Sn}$ at 32A MeV (colours) and 25A MeV (contours) for a central impact parameter.

obtained at 15A MeV, however variances are larger, reflecting the more dissipative dynamics.

It should be noticed that, in the calculations of Ref. [15], as well as in SMF simulations at 15A MeV, the lightest fragment (A1) emerges mainly from the neck region, thus being located at mid-velocity. On the other hand, in the data analysis reported in Ref. [13], the fragment with the largest parallel velocity (F1) has the smallest mass. In SMF simulations, this feature is present, but at higher energy. Indeed, at 23A MeV, owing to increased angular momentum effects, the PLF (or TLF) fragment rotates before it reaches its maximum deformation and a subsequent break-up may take place. Thus this mechanism allows one to test the interplay between the development of surface instabilities and rotational effects, which is governed by the properties of the mean-field interaction. As a consequence, in the case of a PLF break-up for instance, the lightest fragment may emerge with large positive parallel velocity. Thus SMF results point to the occurrence of a reaction mechanism, i.e. neck rupture coupled to angular momentum effects, which could explain the experimental observation. On the other hand, in QMD-like calculations rotational effects could be missing because of the too fast reaction dynamics and the reduced mean-field effects [16, 17].

In the calculations discussed above, the sensitivity to the symmetry energy parametrization has not been explored so far. It would be extremely interesting to extend this kind of investigations to reactions involving neutron-rich (or even exotic) nuclei [18]. Indeed the reaction dynamics could be affected by the neutron-enrichment of the neck region, related to neutron skin effects and/or isospin migration mechanisms [5, 19]. In this case, one would also expect an important sensitivity of the reaction mechanism, and of the features of the emitted fragments, to the isovector terms of the nuclear potential, opening interesting perspectives towards the extraction of new, independent information on the density behavior of the nuclear symmetry energy [20].

IV. SOLUTION OF THE FULL BL EQUATION FOR FERMIONIC SYSTEMS

We now move to discuss recent developments concerning the solution of the BL equation (1) in full phase space. This is the aim of the Boltzmann-Langevin One-Body model (BLOB) [21]. In this approach the conventional Uehling-Uhlenbeck average collision integral is replaced by a similar form where binary collisions, instead of acting only on two test particles a, b , rather involve extended phase-space agglomerates of test particles of equal isospin $A = a_1, a_2, \dots$, $B = b_1, b_2, \dots$, to simulate collisions between nucleon wave packets:

$$\begin{aligned} \bar{I}[f] + \delta I[f] &= g \int \frac{d\mathbf{p}_b}{h^3} \int d\Omega W_{(AB \leftrightarrow CD)} F_{(AB \rightarrow CD)} \\ &= g \int \frac{d\mathbf{p}_b}{h^3} \int d\Omega \langle |v_a - v_b| \frac{d\sigma}{d\Omega} \rangle_{\Sigma} F_{(AB \rightarrow CD)}, \quad (2) \end{aligned}$$

where

$$F_{(AB \rightarrow CD)} = \left[(1-f_A)(1-f_B)f_C f_D - f_A f_B (1-f_C)(1-f_D) \right].$$

At each time interval, the full phase space is scanned for collisions and test-particle agglomerates are redefined in phase-space cells of volume h^3 . The above procedure introduces correlations which are then exploited through a stochastic collision procedure. As a consequence, fluctuations develop spontaneously in phase space, with the correct amplitude, corresponding (at equilibrium) to a variance equal to $f(1-f)$ for volumes containing N_{test} test particles, N_{test} being the number of test particles per nucleon [22]. Since the N_{test} test particles involved in collisions which are not successful can be sorted again in new agglomerates to attempt new collisions, in the same interval of time, the cross section contained in the transition rate W in Eq.(2) corresponds to the nucleon-nucleon cross section divided by N_{test} : $\sigma = \sigma_{NN}/N_{\text{test}}$. We notice that the transition rate $W_{(AB \leftrightarrow CD)}$ is the average of the elementary transition rates $W_{(ab \leftrightarrow cd)}$ over the ensemble Σ of all the couples of test particles belonging to the agglomerates A and B and with velocities v_a and v_b .

The BLOB model applies a precise shape-modulation technique [23] which ensures that the occupancy distribution does not exceed unity in any phase-space point in the final states; this leads to a correct Fermi statistics for the distribution function f , in terms of mean value and variance. The main constraint of the above procedure is to impose a phase-space metric characterised by phase-space cells of volume h^3 . However, the metric of each (momentum and coordinate) stochastic space is unconstrained in general. In the present calculations we impose the maximum compactness for the agglomerates in momentum space which does neither violate Pauli blocking nor energy conservation. However, beyond the present application to Fermi energies, further attention should be paid to the compactness of the wave packets also in coordinate space when dealing with effects like collective flow and stopping, which become relevant at intermediate energies.

The BLOB approach has been tested in the schematic case of nuclear matter contained in a box with periodic boundary conditions. For systems initialized inside the unstable

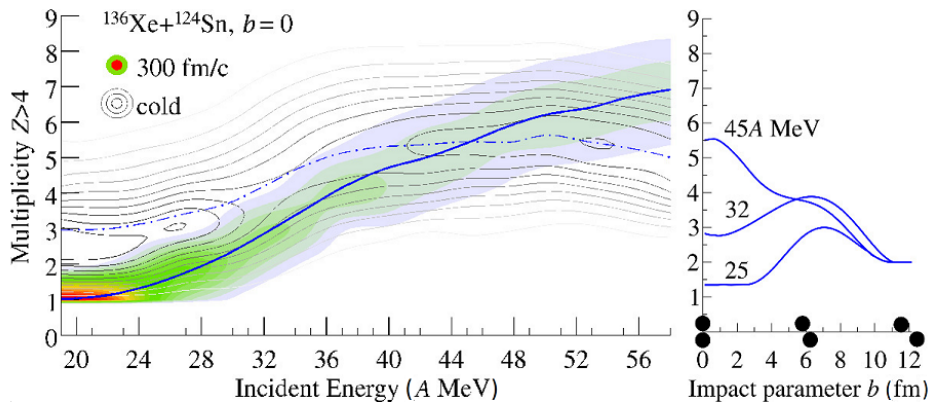


Fig. 4. (Color online) Multiplicity of fragments larger than Be in the reaction $^{136}\text{Xe}+^{124}\text{Sn}$ as a function of the incident energy for a central impact parameter (left panel) and as a function of the impact parameter for 25, 32 and 45 A MeV (right panel).

(spinodal) region of the nuclear matter phase diagram it appears that the stochastic collision integral induces thermal fluctuations which are amplified by the unstable mean-field, in agreement with the standard nuclear dispersion relation [24].

V. FUSION-MULTIFRAGMENTATION COMPETITION IN CENTRAL COLLISIONS

Before turning to discuss the phenomenology of semi-central reactions, we test the BLOB approach for the description of central heavy-ion collisions at Fermi energies, which have been widely investigated in the past years, both from the experimental and theoretical point of view [9, 10]. For convenience (because experimental data exist, measured by the INDRA collaboration [25]), we simulate the reaction $^{136}\text{Xe}+^{124}\text{Sn}$ at 25 and 32 A MeV: in this situation the system is close to the threshold between fusion and multifragmentation (below for 25 A MeV, above for 32 A MeV). The BLOB transport model is employed with the prescription of a soft EoS (with $K = 200$ MeV), a linear Asy-EoS, an in-medium cross section as prescribed in ref. [26], with $N_{\text{test}} = 40$, and with a statistics of 600 events. The dynamics is followed for a time of 300 fm/c.

Figure 3 shows the evolution of the size of inhomogeneities which develop in the potential landscape as a function of time for the two incident energies 25 and 32 A MeV. These inhomogeneities correspond to blobs of matter which, if the dynamics is sufficiently explosive, may eventually leave the system as emitted fragments. At short times, spinodal instabilities tend to split the system in several fragments of comparable size, corresponding approximately to the region of Neon. Later on, this mechanism enters in competition with a protochasticness of partial coalescence determined by the mean-field resilience, which tends to revert the system to a compact shape, and which is more effective for the lowest incident energy.

This picture results in a large variety of exit channels for one given macroscopic initial condition (entrance chan-

nel), ranging from fusion to multifragmentation and passing through very asymmetric configurations with a small fragment multiplicity, eventually binary, and a large size asymmetry. Such intermediate configurations may recall asymmetric fission with the difference that the distribution of momentum transfer could reach large values, more compatible with multifragmentation. These results indicate that the BLOB dynamics is able to describe the development of a large variety of configurations in fragmentation events of dissipative collisions, even at the lowest energy considered (25 A MeV), in agreement with the experimental observations. We notice that the latter result was not reproduced by SMF simulationstochastics, which, owing to the approximate treatment of fluctuations, underestimate fragment production in low-energy reactions [27].

VI. OVERVIEW ON A LANDSCAPE OF EXIT CHANNELS

To present a more general survey, here we extend the set of simulations to a full range of impact parameters, and complete the dynamical calculation with a further decay process of the hot fragments through a statistical evaporation model [28]. We still keep the same reaction, $^{136}\text{Xe}+^{124}\text{Sn}$, but we additionally vary the impact parameter b .

The left panel of Fig. 4 is still restricted to central collisions and shows the evolution of the multiplicity of (primary) fragments larger than Be as a function of the incident energy (coloured distribution with the average marked by a solid line). As expected, fragmentation is favoured as the beam energy increases within the energy window considered here. However, it should be noticed that the distribution of the (final) fragments, obtained after the evaporation process has been considered, reaches a maximum above about 35 A MeV and a fall above 50 A MeV, due to the more and more reduced size of the fragments surviving the evaporation stage.

The right panel of Fig. 4 shows the dependence of the average primary fragment multiplicity as a function of the impact parameter. We observe that, at large incident energies, the maximum corresponds to central collisions, because the mul-

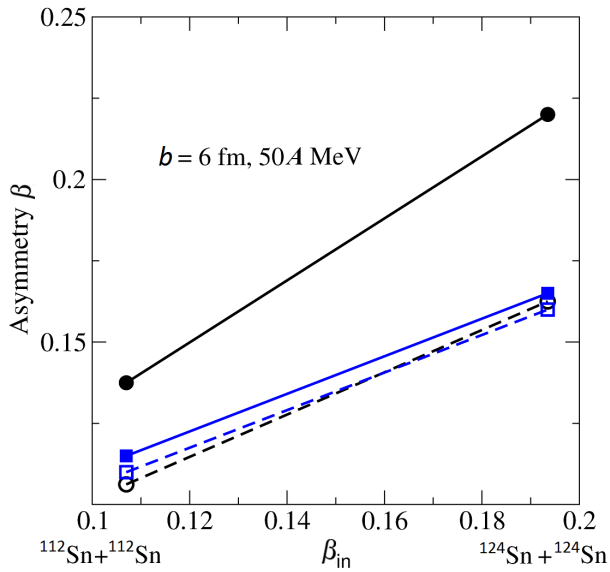


Fig. 5. (Color online) Asymmetry of IMF (circles) and PLF-TLF (squares), as a function of the system initial asymmetry, for two Asy-EOS choices: asystiff (full lines) and asysoft (dashed lines).

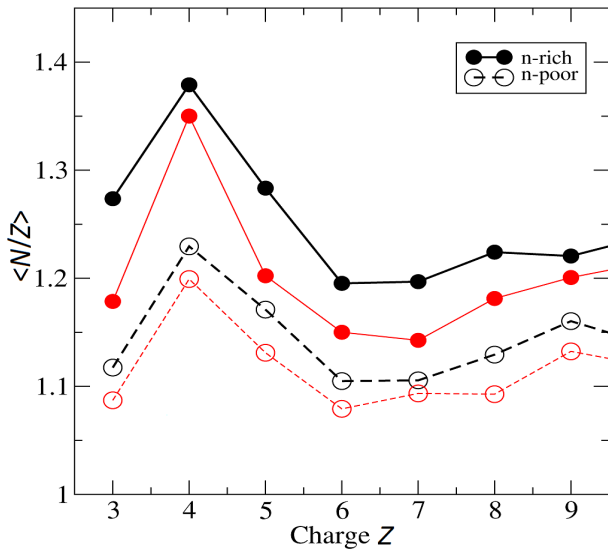


Fig. 6. (Color online) Average N/Z of the neck fragments obtained in the reactions $^{112,124}\text{Sn} + ^{58,64}\text{Ni}$ at 35A MeV, $b = 6-8$ fm. Two parametrizations of the symmetry energy have been employed: asystiff (thick black lines) and asysoft (thin red lines). Full (open) circles correspond to the neutron-rich (poor) system.

tifragmentation channel dominates the reaction cross section. On the other hand, at smaller incident energies, the maximum moves to more peripheral collisions and it is reduced to events with three or four fragments: this indicates that around 30A MeV and for semicentral impact parameters (6 fm) the system oscillates between binary mechanisms and ternary splits, where intermediate mass fragments (IMF) are formed in the neck region. The latter mechanism will be discussed in the next section.

VII. ISOSPIN DYNAMICS IN NECK FRAGMENTATION

It is now quite well established that the largest part of the reaction cross section for dissipative collisions at Fermi energies goes through the *Neck Fragmentation* channel, with IMF directly produced in the interacting zone in semiperipheral collisions, on very short time scales [29]. It is possible to predict interesting isospin transport effects for this fragmentation mechanism since clusters are formed still in a dilute asymmetric matter but always in contact with the regions of the projectile-like and target-like remnants almost at normal densities. In presence of density gradients we expect a neutron flow to the neck clusters and the effect should be larger for a stiffer symmetry energy around saturation [5]. This is shown in Fig. 5, where the asymmetry of the neck region is plotted for two Asy-EOS choices (soft and stiff), compared to the PLF-TLF asymmetry, for SMF simulations of Sn + Sn reactions at 50A MeV, $b = 6$ fm.

This isospin migration effect can be estimated on the basis of simple energy balance considerations. Starting from a residue of mass A_{res} and a neck of mass A_{IMF} we assume that the mass A participating in the isospin exchange is approximately equal to the mass of the neck, while it is small relative to the mass of the residue. This will lead to the asymmetry $(\beta + \Delta\beta)$ of the neck, and to a total asymmetry $\beta_{\text{res}} = [\beta(A_{\text{res}} - A) + (\beta - \Delta\beta)A]/A_{\text{res}} = \beta - \Delta\beta A/A_{\text{res}}$ of the residue, with $\Delta\beta$ to be determined by minimization of the symmetry energy. The corresponding variation of the symmetry energy is equal (apart from a constant) to

$$\Delta E_{\text{sym}} = A_{\text{res}} E_{\text{sym}}(\rho_R) \beta_{\text{res}}^2 + A E_{\text{sym}}(\rho_I) (\beta + \Delta\beta)^2, \quad (3)$$

where ρ_R and ρ_I are the densities of the residue and neck regions, respectively. The minimum of the variation of ΔE_{sym} yields

$$\frac{\beta_{\text{IMF}}}{\beta_{\text{res}}} = \frac{E_{\text{sym}}(\rho_R)}{E_{\text{sym}}(\rho_I)}. \quad (4)$$

From this simple argument the ratio between the IMF and residue asymmetries should depend only on symmetry energy properties and, in particular, on the difference of the symmetry energy between the residue and the neck regions, as appropriate for isospin migration. It should also be larger than one, even more so for the asystiff than for the asysoft EOS, as indicated by Fig. 5.

The isospin migration mechanism is responsible for the emission of rather “exotic” (neutron-rich) fragments from the neck region. Moreover, as discussed above, the fragment N/Z is nicely dependent on the parametrization employed for the symmetry potential. The latter effect has been recently investigated also in the context of the BLOB model, for $^{112,124}\text{Sn} + ^{58,64}\text{Ni}$ reactions at 35A MeV, $b = 6-8$ fm, for which recent experimental data exist [19]. Fig. 6 shows the average N/Z of the fragments emitted from the neck region, as a function of their charge, for the two reactions considered and two parametrizations of the symmetry energy (stiff and

soft). Quite neutron-rich fragments are produced, especially in the stiff case, in good agreement with the experimental data [19].

VIII. CONCLUSION

We have undertaken an analysis of new fragmentation mode, on which recent experimental investigations have been concentrated, which may develop in low and Fermi energy heavy ion collisions. At low energies, the possibility of observing ternary breakup processes of dynamical origin is explored within the SMF model, looking at the concurrent

role of surface mean-field instabilities, dissipative and angular momentum effects. Indeed large quadrupole and octupole deformation effects are developing in binary exit channels of semi-central reactions, which may lead to a subsequent breakup of the PLF/TLF fragments. At Fermi energies IMF are directly emitted from the low-density neck region. In reactions between neutron-rich systems, we observe a neutron flow towards the neck, yielding quite exotic primary fragments. This effect, also confirmed by calculations with the new BLOB model, nicely depends on the stiffness of the symmetry potential, allowing one to get new information on the low-density behavior of the nuclear symmetry energy.

-
- [1] Danielewicz P, Lacey R and Lynch W G. Determination of the equation of state of dense matter. *Science*, 2002, **298**: 1592–1596. DOI: [10.1126/science.1078070](https://doi.org/10.1126/science.1078070)
- [2] Lattimer J M and Prakash M. Neutron star observations: Prognosis for equation of state constraints. *Phys Rep*, 2007, **442**: 109–165. DOI: [10.1016/j.physrep.2007.02.003](https://doi.org/10.1016/j.physrep.2007.02.003)
- [3] Burrello S, Colonna M and Matera F. Pairing effects on spinodal decomposition of asymmetric nuclear matter. *Phys Rev C*, 2014, **89**: 057604. DOI: [10.1103/PhysRevC.89.057604](https://doi.org/10.1103/PhysRevC.89.057604)
- [4] Piekarewicz J, Agrawal B K, Colò G, *et al.* Electric dipole polarizability and the neutron skin. *Phys Rev C*, 2012, **85**: 041302. DOI: [10.1103/PhysRevC.85.041302](https://doi.org/10.1103/PhysRevC.85.041302)
- [5] Baran V, Colonna M, Greco V, *et al.* Reaction dynamics with exotic nuclei. *Phys Rep*, 2005, **410**: 335–476. DOI: [10.1016/j.physrep.2004.12.004](https://doi.org/10.1016/j.physrep.2004.12.004)
- [6] Ayik S, Gregoire C. Fluctuations of single-particle density in nuclear collisions. *Phys Lett B*, 1998, **212**: 269–272. DOI: [10.1016/0370-2693\(88\)91315-9](https://doi.org/10.1016/0370-2693(88)91315-9)
- [7] Li B A, Das C B, Das Gupta S, *et al.* Momentum dependence of the symmetry potential and nuclear reactions induced by neutron-rich nuclei at RIA. *Phys Rev C*, 2004, **69**: 011603(R). DOI: [10.1103/PhysRevC.69.011603](https://doi.org/10.1103/PhysRevC.69.011603)
- [8] Colonna M, Di Toro M, Guarnera A, *et al.* Fluctuations and dynamical instabilities in heavy-ion reactions. *Nucl Phys A*, 1998, **642**: 449–460. DOI: [10.1016/S0375-9474\(98\)00542-9](https://doi.org/10.1016/S0375-9474(98)00542-9)
- [9] Chomaz P, Colonna M and Randrup J. Nuclear spinodal fragmentation. *Phys Rep*, 2004, **389**: 263–440. DOI: [10.1016/j.physrep.2003.09.006](https://doi.org/10.1016/j.physrep.2003.09.006)
- [10] Borderie B and Rivet M F. Nuclear multifragmentation and phase transition for hot nuclei. *Prog Part Nucl Phys*, 2008, **61** (Book Series): 551–601, and refs. therein. DOI: [10.1016/j.pnpnp.2008.01.003](https://doi.org/10.1016/j.pnpnp.2008.01.003)
- [11] Guarnera A, Colonna M and Chomaz Ph. 3D stochastic mean-field simulations of the spinodal fragmentation of dilute nuclei. *Phys Lett B*, 1996, **373**: 267–274. DOI: [10.1016/0370-2693\(96\)00152-9](https://doi.org/10.1016/0370-2693(96)00152-9)
- [12] Skwira-Chalot I, Siwek-Wilczyńska K, Wilczyński J, *et al.* Dynamical evolution of the $^{197}\text{Au} + ^{197}\text{Au}$ system at 15 MeV/nucleon. *Int J Mod Phys E*, 2006, **15**: 495–499. DOI: [10.1142/S0218301306004429](https://doi.org/10.1142/S0218301306004429)
- [13] Wilczyński J, Skwira-Chalot I, Siwek-Wilczyńska K, *et al.* Observation of fast collinear partitioning of the $^{197}\text{Au} + ^{197}\text{Au}$ system into three and four fragments of comparable size. *Phys Rev C*, 2010, **81**: 024605. DOI: [10.1103/PhysRevC.81.024605](https://doi.org/10.1103/PhysRevC.81.024605)
- [14] Cap T, Siwek-Wilczyńska K, Skwira-Chalot I, *et al.* Aligned ternary partitioning of the $^{197}\text{Au} + ^{197}\text{Au}$ system at 23A MeV beam energy. *Phys Scripta*, 2014, **89**: 054005. DOI: [10.1088/0031-8949/89/5/054005](https://doi.org/10.1088/0031-8949/89/5/054005)
- [15] Li Y, Yan S, Jiang X, *et al.* Dynamical effects in heavy-ion induced ternary breakup. *Nucl Phys A*, 2013, **902**: 1–20. DOI: [10.1016/j.nuclphysa.2013.02.015](https://doi.org/10.1016/j.nuclphysa.2013.02.015)
- [16] Colonna M, Ono A and Rizzo J. Fragmentation paths in dynamical models. *Phys Rev C*, 2010, **82**: 054613. DOI: [10.1103/PhysRevC.82.054613](https://doi.org/10.1103/PhysRevC.82.054613)
- [17] Rizzo J, Colonna M and Ono A. Comparison of multifragmentation dynamical models. *Phys Rev C*, 2007, **76**: 024611. DOI: [10.1103/PhysRevC.76.024611](https://doi.org/10.1103/PhysRevC.76.024611)
- [18] Cammarata P, Colonna M, Bonasera A, *et al.* Sifting through the remnants of heavy-ion collisions for observables sensitive to the nuclear equation of state. *Nucl Instrum Meth A*, 2014, **761**: 1–6. DOI: [10.1016/j.nima.2014.05.108](https://doi.org/10.1016/j.nima.2014.05.108)
- [19] De Filippo E, Pagano A, Russotto P, *et al.* Correlations between emission timescale of fragments and isospin dynamics in $^{124}\text{Sn} + ^{64}\text{Ni}$ and $^{112}\text{Sn} + ^{58}\text{Ni}$ reactions at 35A MeV. *Phys Rev C*, 2012, **86**: 014610. DOI: [10.1103/PhysRevC.86.014610](https://doi.org/10.1103/PhysRevC.86.014610)
- [20] Li B A, Ramos À, Verde G, *et al.* Topical issue on nuclear symmetry energy. *Eur Phys J A*, 2014, **50**: 9–11. DOI: [10.1140/epja/i2014-14009-x](https://doi.org/10.1140/epja/i2014-14009-x)
- [21] Napolitani P and Colonna M. Bifurcations in Boltzmann–Langevin one body dynamics for fermionic systems. *Phys Lett B*, 2013, **726**: 382–386. DOI: [10.1016/j.physletb.2013.08.005](https://doi.org/10.1016/j.physletb.2013.08.005)
- [22] Rizzo J, Chomaz Ph and Colonna M. A new approach to solve the Boltzmann–Langevin equation for fermionic systems. *Nucl Phys A*, 2008, **806**: 40–64. DOI: [10.1016/j.nuclphysa.2008.02.304](https://doi.org/10.1016/j.nuclphysa.2008.02.304)
- [23] Napolitani P and Colonna M. Boltzmann–Langevin one-body dynamics for fermionic systems. *Eur Phys J Web of Conf*, 2012, **31**: 00027–00033. DOI: [10.1051/epjconf/20123100027](https://doi.org/10.1051/epjconf/20123100027)
- [24] Colonna M and Chomaz Ph. Unstable infinite nuclear matter in stochastic mean field approach. *Phys Rev C*, 1994, **49**: 1908–1916. DOI: [10.1103/PhysRevC.49.1908](https://doi.org/10.1103/PhysRevC.49.1908)
- [25] Gagnon-Moisan F, Galichet E, Rivet M F, *et al.* New isospin effects in central heavy-ion collisions at Fermi energies. *Phys Rev C*, 2012, **86**: 044617. DOI: [10.1103/PhysRevC.86.044617](https://doi.org/10.1103/PhysRevC.86.044617)
- [26] Danielewicz P. Hadronic transport models. *Acta Phys Pol B*, 2002, **33**: 45–64; Coupland D D S, Lynch W G, Tsang M B, *et al.* Influence of transport variables on isospin transport ratios *Phys Rev C*, 2011, **84**: 054603. DOI: [10.1103/Phys-](https://doi.org/10.1103/Phys-)

- [RevC.84.054603](#)
- [27] Bonnet E, Colonna M, Chbihi A, *et al.* Investigation of collective radial expansion and stopping in heavy ion collisions at Fermi energies. *Phys Rev C*, 2014, **89**: 034608. DOI: [10.1103/PhysRevC.89.034608](#)
- [28] Durand D. An event generator for the study of nuclear collisions in the Fermi energy domain (I). Formalism and first applications. *Nucl Phys A*, 1992, **541**: 266–298. DOI: [10.1016/0375-9474\(92\)90097-4](#)
- [29] De Filippo E, Pagano A, Wilczynski J, *et al.* Time sequence and time scale of intermediate mass fragment emission. *Phys Rev C*, 2005, **71**: 044602. DOI: [10.1103/PhysRevC.71.044602](#)